SANDIA REPORT
SAND20107014
Unlimited Release
Printed October 2010

Structural Simulations of Nanomaterials Self-Assembled from Ionic Macrocycles

Craig J. Medforth and Frank B. van Swol

Prepared by
Sandia National Laboratories
Albuquerque, New Mexico 87185 and Livermore, California 94550

Sandia National Laboratories is a multi-program laboratory managed and operated by Sandia Corporation, a wholly owned subsidiary of Lockheed Martin Corporation, for the U.S. Department of Energy's National Nuclear Security Administration under contract DE-AC04-94AL85000.

Issued by Sandia National Laboratories, operated for the United States Department of Energy by Sandia Corporation.

Available to DOE and DOE contractors from
U.S. Department of Energy
Office of Scientific and Technical Information
P.O. Box 62
Oak Ridge, TN 37831

Telephone: (865) 576-8401
Facsimile: (865) 576-5728
E-Mail: reports@adonis.osti.gov
Online ordering: http://www.osti.gov/bridge

Available to the public from
U.S. Department of Commerce
National Technical Information Service
5285 Port Royal Rd.
Springfield, VA 22161

Telephone: (800) 553-6847
Facsimile: (703) 605-6900
E-Mail: orders@ntis.fedworld.gov
Online order: http://www.ntis.gov/help/ordermethods.asp?loc=7-4-0#online

SAND2010-7014
Unlimited Release
Printed October 2010

Structural Simulations of Nanomaterials Self-Assembled from Ionic Macrocycles

Craig J. Medforth

Center for Micro-Engineered Materials
The University of New Mexico
1001 University Blvd, SE
Albuquerque, NM 87106

Frank van Swol
Department 1814
Sandia National Laboratories
P.O. Box 5800
Albuquerque, New Mexico 87185-MS1419

Abstract

Recent research at Sandia has discovered a new class of organic binary ionic solids with tunable optical, electronic, and photochemical properties. These nanomaterials, consisting of a novel class of organic binary ionic solids, are currently being developed at Sandia for applications in batteries, supercapacitors, and solar energy technologies. They are composed of self-assembled oligomeric arrays of very large anions and large cations, but their crucial internal arrangement is thus far unknown. This report describes a) the development of a relevant model of nonconvex particles decorated with ions interacting through short-ranged Yukawa potentials, and b) the results of initial Monte Carlo simulations of the self-assembly binary ionic solids.

ACKNOWLEDGMENTS

The authors benefitted from, and are grateful for, many in-depth discussions with Dr. John A. Shelnutt.

CONTENTS

1. Introduction 7

2. Methods 8
   2.1 Models of Hard Convex Particles 8
      2.1.1 Spherical Particles 8
      2.1.2 Nonspherical Particles 9
      2.1.3 Composite spheres as Nonspherical Particles 10
      2.1.4 Some Conventions: Dimensionless Quantities 10
   2.2 Models of Composite Particles 11
   2.3 Charge interactions 12

3. Results 13
   3.1 Derivation of the particles used in the simulation. 13
   3.2 Construction, relative energies and packing fractions of crystal lattices 14
   3.3 Simulations of the self-assembly process. 15

4. Conclusions 16

5. References 18

Distribution 19

NOMENCLATURE

CCDC	Cambridge Crystallographic Data Center
$f(\sigma)$	probability density function of diameters σ
k	Boltzmann's constant
L_α	length of side α of a parallelepiped
M	number of components
MC	Monte Carlo
MD	molecular dynamics
N	number of particles
r_{ij}	distance between particles I and j
p	pressure
q_i	charge of ion i
T	temperature
TPP	tetraphenylporphyrin
TPPS	tetrakis(4-sulfonatophenyl)porphyrin
TCNQ	tetracyanoquinodimethane
TTF	tetrathiafulvalene
TTF-TCNQ	strong charge-transfer complex of TTF and TCNQ
V	volume
v_i	volume of particle i

α_{ij}	nonadditivity parameter of the ij interaction
ϕ	potential energy function
η	packing fraction
κ	inverse screening length
ρ	= N/V, particle density
σ	hard sphere diameter

1. INTRODUCTION

Detailed information about the internal structures of nanomaterials can be crucial for understanding their function. In the case of the organic binary ionic solids that will be studied in this project, knowledge of the internal structure (i.e., the arrangement of the organic ions) is especially important because interactions between the organic ions control key properties of the materials such as light absorption, charge separation, and electron transfer. However, obtaining such detailed information for nanomaterials is a non-trivial problem, and in many cases even indirect methods such as spectroscopic probes provide only limited insights.

Recent research at Sandia has discovered a new class of organic binary ionic solids with tunable optical, electronic, and photochemical properties. These novel materials are currently being developed at Sandia for applications in batteries, supercapacitors, and solar energy technologies. They are composed of self-assembled oligomeric arrays of large anions and large cations such as crown ethers, dye molecules (e.g., phthalocyanines), or other compounds with highly variable molecular structures. Currently, materials are prepared by ionic self-assembly of oppositely charged organic dye molecules that are typically 2 x 2 nm on edge and approximately 0.5 nm thick. The macrocycles have ionic substituents at their corners and can have metal ions complexed to the center of the macrocycle (see Figure 1a). The electrostatic interaction of the positive and negative charges drives the formation of the materials, often producing nanostructures (see Figure 1b) but sometimes microstructures with nanoscale features.

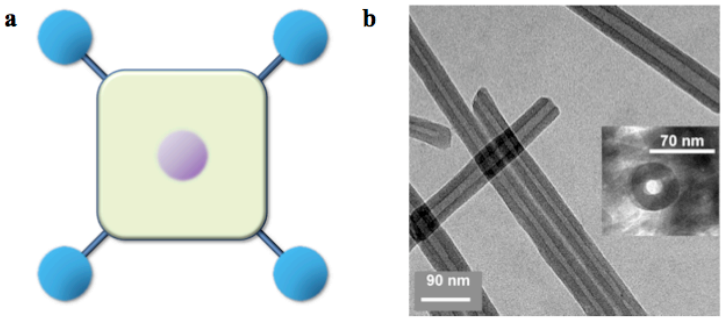

Figure 1. (a) Model of an organic macrocycle (green) with four peripheral charge centers representing the ionic substituents (blue) and a central charge representing the complexed metal ion (purple). (b) Transmission electron microscope image of nanotubes obtained by the self-assembly of two oppositely charge organic ions. In this case, the organic ions are dye molecules and the nanotubes are photocatalytically active. The inset shows a tube caught in an end-on orientation, confirming that the tubes are hollow.

Ionic interactions direct the self-assembly process to produce a framework that positions the organic moieties. This then enables tailoring of the electronic and optical properties of the materials by modulating collective interactions between the organic moieties. There is little understanding of the internal structures and properties of these novel materials because of the well-known difficulties inherent in direct structural characterization of nanomaterials by X-ray crystallography. The goal of this work is to develop a platform for predictive simulations of the structures of these new organic binary ionic materials using Monte Carlo methods.

2. METHODS

Monte Carlo (MC) and Molecular Dynamics (MD) simulation techniques have applications in numerous areas involving hard convex particles, including:

1. fluid- and solid-phase behavior of atomic and polymeric systems
2. phase-behavior of self-assembling mixtures
3. dynamics and packing of powders (granular materials)
4. generation of random close-packings of mixtures of hard particles

Although seemingly wide-ranging, these areas of interest are in fact often reasonably similar when viewed from a purely technical point of view. That is, all these areas share the need for a capability to generate valid, i.e. overlap free, configurations of some kind of hard convex bodies. The differences mainly concern the type of statistical mechanical ensemble that applies to each case, and the equilibrium versus non-equilibrium aspects. For example, a crystallization project of hard spheres will typically involve equilibrium MD or MC simulations in the canonical or NVT (constant number of particles, N, constant volume, V, and constant temperature, T) ensemble that allow the calculation of the absolute free energy of the solid phase, as well as MD simulations that monitor the nucleation and growth of a hard sphere crystal, i.e. the approach to equilibrium. On the other hand, to generate a random close-packed configuration of collections of hard spheres one would run an MD simulation of growing spheres (spheres whose diameter is time-dependent) until the system is thoroughly jammed, with all spheres touching. Similarly, powder-packing in a container might require one to run a MD simulation of inelastic spheres in gravity, while a packing of hard cubes would be generated by using MC in the constant pressure or NpT ensemble with the pressure, p, set to infinity.

This report gives an overview of the enhancement of the basic capabilities of HSMIX, a Fortran code specifically developed to simulate a variety of different models spanning the range indicated above, and running on a variety of platforms including under Mac OS [1]. The report provides a description of the relevant general approach as well as important strategies underlying HSMIX and includes references to the existing literature. Features unique to the simulation of ionic macrocycles are treated in more detail.

2.1 Models of Hard Convex Particles

2.1.1 Spherical Particles

Each model system is defined by specifying the Hamiltonian which expresses the interaction pair- potentials acting between the different particles. For so-called hard particles these are the simplest of all, namely the particles experience an infinite potential energy when they overlap, and zero potential energy otherwise. Thus for two hard spheres of diameter σ_i and σ_j we have

$$\phi(r_{ij}) = \begin{cases} 0 & r_{ij} > \sigma_{ij} \\ \infty & r_{ij} < \sigma_{ij} \end{cases} \qquad (1)$$

where $\sigma_{ij} = \alpha_{ij}(\sigma_i + \sigma_j)/2$ with α_{ij} a coefficient that controls the additivity of the interaction. If $\alpha_{ij} > 1$ then the two particles appear larger than their arithmetic mean and hence experience an enhanced repulsion over the simple additive spheres. On the other hand, if $\alpha_{ij} < 1$ a reduced repulsion results. The parameter α allows one to promote or discourage mixing of various species in a mixture. This simple pair-potential leads to significant simplifications in the statistical mechanics of hard particle systems. Foremost amongst these is the fact that the phase diagram of non-additive fluids is a function of the density (or packing fraction) only, and *not* of the temperature (T). This follows immediately from the fact that for hard particles the Boltzmann factor ($\exp(-\varphi/kT)$) reduces to either 0 or 1, and is hence independent of T. As a consequence, hard particle systems only have one single isotherm as all the properties scale linearly with the kinetic energy, i.e. T.

2.1.2 Nonspherical Particles

For hard spheres the overlap criterion, expressed in Eq. 1, amounts to a simple test, merely comparing the interparticle distance to the diameters. This test can be executed quickly on a computer. Nonspherical particles on the other hand are much more difficult, and the algorithms required to apply the overlap criterion are considerably more complex. In addition, whereas both MD and MC are readily used for spheres, MD becomes extremely challenging for nonspherical particles, and without very special extra care certainly less efficient. Of course, non-spherical particles constitute a potentially huge class, but in practice it is often narrowed down considerably. Thus, the nonspherical particle shapes that have been considered in the past (starting in the 1980s) still possess a high degree of symmetry. They include spheroids of revolution, spherocylinders (cylinders with a hemispherical cap), and cylinders with flat surfaces. These particular choices have been considered primarily because of the (relative) ease of developing and implementing an overlap criterion and further for their application in the area of liquid-crystals. Inspired by developments in granular materials we were previously motivated to take the next step and developed an algorithm for mixtures of parallelepipeds, block shaped particles consisting of 8 vertices and three sets of parallel faces. These objects are fully defined by providing three unit edge (or body) vectors (a, b, c) and three edge lengths L_a, L_b, and L_c. Alternatively, following the notation commonly used to categorize Bravais lattices, one can specify three lengths and three angles (α, β, γ).

To simulate parallelepipeds we are currently restricted to the MC technique, and an efficient overlap detection algorithm. Whereas in two dimensions the overlap of parallelograms requires at least one particle vertex to lie inside the other particle, in three dimensions this is not the case. The algorithm we have developed considers the intersection of all possible pairs of edges of particle i and faces of particle j, and vice versa. In the worst-case scenario this could amount to checking 2x12x6 = 144 intersections! With each intersection problem being already far more computationally intensive than a simple check for sphere overlap it is easy to see that a simulation of parallelepiped particles is considerably more complex than a system of spheres. This probably goes a long way towards explaining why this kind of simulation has not been attempted previously.

2.1.3 Composite spheres as Nonspherical Particles

Given that spheres are convenient computational shapes it is natural to consider the possibility of building composite particles, i.e. particles that are each composed of a (preferably) small set of connected spheres. This is indeed a powerful strategy, and to a large extent also part of the HSMIX capabilities. For reasons of computational efficiency and to maintain a model that has no temperature dependence we have implemented composite particles that are clusters or polymer chains of tethered spheres. A tether is a string (as opposed to a spring) of finite extension l that ties two spheres together, and forces them to stay linked. As long as the sphere centers are closer than l, the potential will be zero. Otherwise the potential is infinite. Notice that technically speaking the tether is equivalent to a square-well potential of infinite depth. The tether length should be chosen small enough, compared to the particle diameters, such that one avoids issues related to the crossing of distinct tethers. In practice tethers of 0.1σ are a typical choice

2.1.4 Some Conventions: Dimensionless Quantities

As stated before hard particle systems have phase diagrams that consist of just a single isotherm, depending only on the (number) density. Thus for monodisperse hard spheres all properties depend on the density $\rho = N/V$, where N is the number of particles and V is the volume of the MD box. It is customary to select the sphere diameter, σ, as the unit of length and to define a dimensionless density (sometimes denoted as the reduced density ρ^*) which in 3D is $\rho\sigma^3 = N\sigma^3/V$. A derived quantity is the packing fraction, η, (or in some parts of the literature φ). For monodisperse hard spheres we have

$$\eta = \frac{N}{V}\frac{\pi\sigma^3}{6} \qquad (2)$$

The packing fraction is, as the name suggest, the fraction of the volume that is occupied by the spheres. Recall that $\pi\sigma 3/6$ is the volume of of a sphere of diameter σ. This interpretation assumes, of course, that the spheres are nonoverlapping. Otherwise it is an upper bound.
To preserve the above interpretation of packing fraction, for an M-component mixtures of spheres the expressions must become

$$\begin{aligned}\eta &= \frac{1}{V}\sum_i^M N_i \frac{\pi\sigma_i^3}{6} \\ &= \frac{\sigma_1^3}{V}\sum_i^M N_i \frac{\pi R_i^3}{6}\end{aligned} \qquad (3)$$

where Ni denotes the number of spheres of species i of diameter σi. The diameter ratios are $\sigma i/\sigma 1$. Analogously, for nonspherical particles we have, in terms of the volume , vi, of species i,

$$\eta = \frac{1}{V}\sum_i^M N_i v_i \qquad (4)$$

It is instructive to re-arrange expression 4, and rewrite it with the help of the molefractions $xi \equiv N_i/N$ as:

$$\eta = \frac{N}{V}\frac{\pi}{6}\sum_{i}^{M} x_i \sigma_i^3 \qquad (5)$$

This allows a straightforward generalization to polydisperse mixtures. First, we recognize that the molefraction xi is essentially the probability density, f(σi) for finding a sphere of diameter σi. Then, upon re-expressing the packing fraction more formally in terms of the probability density distribution, we obtain an expression that is valid for any mixture, polydisperse or discrete.

$$\begin{aligned}\eta &= \frac{N}{V}\frac{\pi}{6}\int_0^\infty d\sigma f(\sigma)\sigma^3 \\ &= \frac{N}{V}\frac{\pi}{6}\langle\sigma^3\rangle\end{aligned} \qquad (6)$$

where < σ3 > is the third moment of the particle size distribution (to be distinguished from < σ >3, the average diameter cubed)

2.2 Models of Composite Particles

In this section we will address composite particles, in particular, particles that result from combining several convex particles. Perhaps the simplest example of this results when we build a diatom out of two spheres that can be overlapping, touching or with centers farther apart or less apart than the sum of the two radii. The combining of particles implies that the subparticles are held together by some type of unbreakable bond. This bond can take various forms. It can be rigid, a spring, or a finite extension tether. The objective of composite particles is to represent more complex shapes. In this report we will focus on rigid bonds.

To enable an adequate exploration of both the equilibrium phase behavior and the kinetics of binary ionic systems requires a judicious choice of a simplified model that contains the essential physics. The crucial elements defining the organic ions that must be represented are the overall shape of the organic ion (i.e., a thin square) and the ionic groups (both position and charge). To capture all of these characteristics, we will employ a model representing the organic ions by thin hard parallelepipeds decorated with up to 5 charge centers (see Figure 1a). Each charge center is composed of a hard sphere with an electronic charge at its center. Four charges centers are located at the corners (corresponding to the ionic substituents) and a final charge is located at the center of mass of the molecule (corresponding to a complexed metal ion). Complete flexibility exists regarding the shape and size of the parallelepiped as well as the value of the charges. In addition to the excluded volume interactions between parallelepipeds and spheres there exist charge-charge interactions. The latter will be represented by an effective (Yukawa) pair-potential which captures the screened Coulombic interactions. We have implemented the above model in a combined Monte-Carlo/Molecular dynamics code that was previously developed to study the behavior of general mixtures of hard convex particles. As an aside, our ionic model also has all the necessary features to study other ionic systems of interest, such as ionic liquids.

The simulations will be performed employing the Monte Carlo method in both the constant volume (NVT) and constant pressure (NpT) ensembles using a stoichiometric ratio of the binary components. This approach will enable the prediction of the solid structure as a function of charge distribution, size and shape, temperature and pressure. The self-assembly process of the binary ionic solid can be studied by using the NVT ensemble and preparing the simulation system at a fixed density that lies in between the densities of the coexisting solid and dilute phase. To obtain time-dependent information about the self-assembly process we switch in the future from Metropolis Monte Carlo to Brownian dynamics. This requires estimates or experimental information about the translational and rotational diffusion coefficients. We have previously done this for a system of hard rod colloids.

2.3 Charge interactions

The ionic macrocycles introduced above experience coulombic interactions between the ions. The Coulomb potential between two ions of (partial) charge q_i and q_j is proportional to the inverse of the distance between them, i.e., $\phi(r_{ij}) \sim q_i\, q_j\, /r_{ij}$. This interaction is positive (i.e., repulsive) for like charges, $q_i\, q_j>0$, and attractive otherwise. The Coulomb interaction is very long range, it is the slowest decay encountered. In ionic systems this interplay between repulsive and attractive interactions leads to charge ordering: ions at short-range find themselves primarily surrounded by the opposite charged ion [3]. In the solid phase this leads to the familiar ionic crystals such as halite (or rock salt, NaCl). The charge ordering effect in a dense fluid is also of very long range.

The long-range nature of charge ordering is not, as is commonly implicitly assumed, the consequence of the long-range Coulomb force. In fact, it is the consequence of the positive/negative nature of the ionic system, which causes an interplay between favorable attractions and unfavorable repulsions. Short-range interaction models can give rise to the very same charge ordering. A powerful example is that of a non-additive hard sphere AB mixture, where the AA and BB interactions are defined to be less favorable then the AB interaction. For a binary non-additive hard sphere mixture this is accomplished by employing $\sigma_{ij} = \alpha_{ij}(\sigma_i + \sigma_j)/2$, with $\alpha_{AB}=1$ and $\alpha_{AA}= \alpha_{BB}>1$. Remarkably, such a simple system has been shown to display all the simple salt crystal structures [2].

In order to study ionic macrocycles of the complex shape defined above it is advantageous to consider a short-range version of an ionic interaction. For this we choose the familiar Yukawa interaction

$$\phi(r_{ij}) = \frac{\varepsilon q_i q_j e^{-\kappa r_{ij}}}{r_{ij}}$$

Here, $1/\kappa$ denotes a decay-length, and ε is a constant that denotes the strength of the interaction and sets the energy scale. The Yukawa potential has a convenient functional form, and arises naturally in the context of screened Coulomb interactions, such as are encountered in suspension of colloidal particles. As is common, the actual implementation we use is the cut-and-shifted

form of the Yukawa potential, where a cut-off distance r_c is used and the potential is shifted to zero at r= r_c to make the potential (but not the force) continues at r_c.

3. RESULTS

3.1 Derivation of the particles used in the simulation.

Simulations of the self-assembled porphyrin nanostructures were undertaken using a structure derived from the crystal structure of the common synthetic porphyrin 5,10,15,20-tetraphenylporphyrin (H_2TPP). The coordinates of the structure (reference code TPHPOR01) were taken from the Cambridge Crystallographic Data Center (CCDC) [4]. The structure of the porphyrin molecule is shown in Figure 2, together with a space-filling model generated from the coordinates.

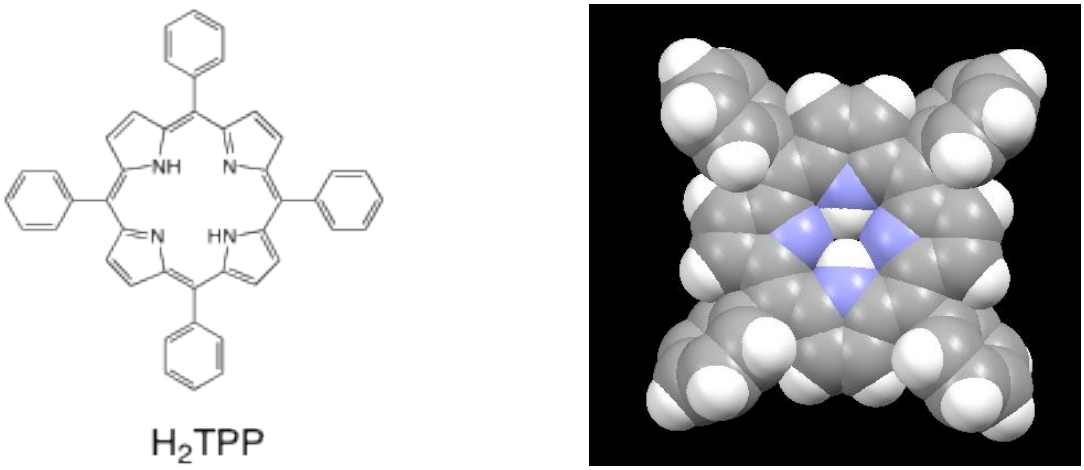

Figure 2. Chemical structure of H2TPP and a space-filling model of a crystal structure of H2TPP.

A porphyrin ion was modeled as a block with spheres at the four corners representing the substituents on the macrocycle. Most of the porphyrins used in the experimental ionic self-assembly studies are variants of TPP with ionic groups located on the porphyrin macrocycle [5-7]. Examples include T(NMe4Py)P (positively charged) and TPPS (negatively charged) (Figure 3). The dimensions of the block required to encompass the porphyrin ring of H_2TPP was determined to be 12.5 x 3.4 Å, based on the measured width of the block plus twice the van der Waals radius of a hydrogen atom. The thickness of the block was set at twice the van der Waals radius of a carbon atom. The diameter of the charged spheres representing the ionic substituents was set to 6.6 Å, derived from the width of a phenyl group (4.2 Å) plus twice the van der Waals radius of a hydrogen atom.

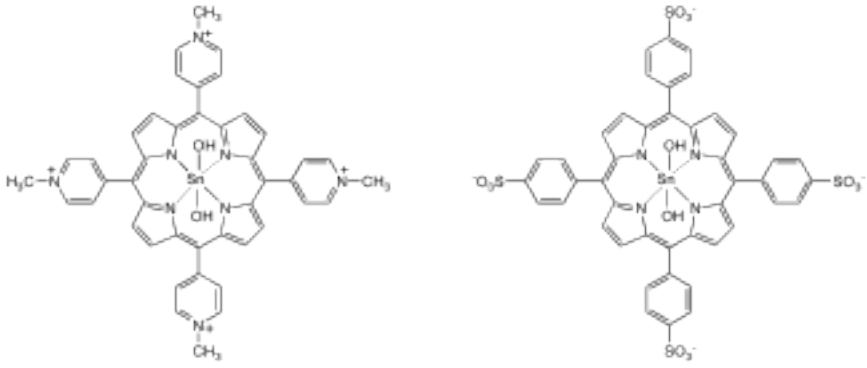

Figure 3. Chemical structure of the tin complexes of the charged porphyrins T(NMe4Py)P (4+) and TPPS (4-).

3.2 Construction, relative energies and packing fractions of crystal lattices

Lattices were generated from the structure described in Section 3.1. Oppositely charged porphyrins (+4 or -4) were positioned using fractional coordinates such that lattices of any desired size could be produced. Figure 4 shows some of the different ways in which a fully interleaved lattice composed of 192 porphyrins was visualized. This array consists of 96 porphyrins with a charge of +4 (red) and 96 porphyrins with a charge of -4 (grey). Each charged sphere is surrounded by four oppositely charged spheres, two in the plane of the porphyrin ring (Figure 4a, defined as the x,y plane) and one each from the porphyrin ions above and below (Figure 4b, defined as the z axis). The boundaries of the simulation box are shown by the white lines in Figure 4.

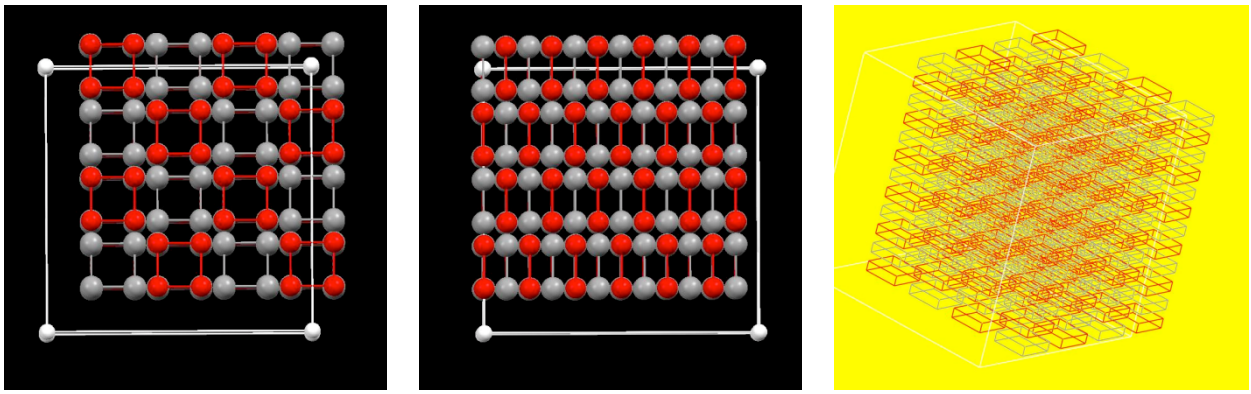

Figure 4. Different ways of visualizing an interleaved lattice composed of oppositely charged porphyrin ions (red and grey): (a) and (b) porphyrins are shown as plates with the ionic substituents as spheres; (c) with solid blocks representing the porphyrins and the spheres not shown

A brief survey was conducted to determine the relative energies of different lattice structures. Lattices were generated with a range of packing motifs such as the fully interleaved pattern shown in Figure 4, segregated columns of porphyrins with the same charge (Figure 5a), offset

stacks of porphyrin (Figure 5b), and z- or x,y-layered (Figure 5c) structures (in the layered structures, the layers consist of porphyrins of the same charge). The segregated and interleaved structures are of particular interest because of their relevance to models of conductivity in classical donor-acceptor solids such as TTF-TCNQ [5], and the potential use of the binary porphyrin solids in applications such as artificial photosynthesis. The distances between the charges were manually optimized to obtain the lowest energy structure for each motif. The larger number of structural parameters that could be varied for the lower symmetry offset stacking structure prevented a definitive determination of the lowest energy structure for this motif. Overall, the lowest energy motif was found to be the fully interleaved structures shown in Figure 4, for which the energy per particle was -3.295. Physical reasonable structures with low energies were also found for the offset stack (-3.101), x,y-layered (-2.569) and segregated (-2.230) structures. For comparison, structures with randomly oriented porphyrins (generated by extended NVT runs of the ordered lattice structures at high temperatures) had energies per particle as low as -3.1 (depending upon the packing fraction).

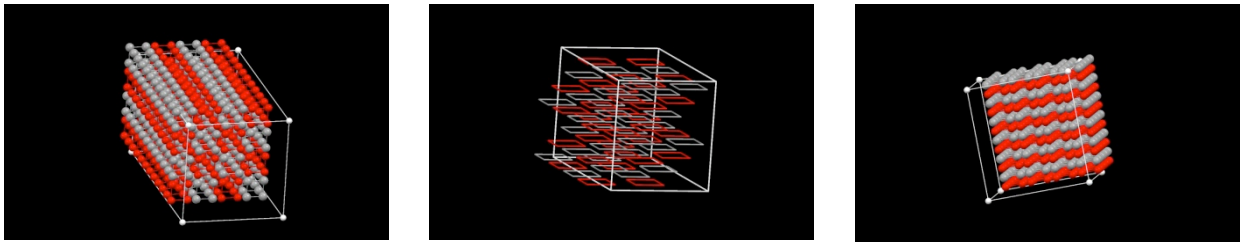

Figure 5. Different lattices generated for oppositely charged porphyrins: (a) segregated columns, (b) offset stacks, (c) x,y-layered.

For the cases examined, the packing fraction was inversely correlated with the energy per particle for the structure. For example, the fully interleaved structure gave the highest packing fraction (xsi value) of 0.22. Note that this xsi value is based on the volume of the blocks i.e., the sphere volume was not included in the calculation, so the true xsi value will be higher. The offset stack structure had a packing fraction of 0.21 and the x,y-layered structure a xsi value of 0.16 The segregated structure is more complicated because the repulsive interactions between the like-charged porphyrins within a column decrease significantly as the packing fraction is reduced, but a some point the structure becomes physically unrealistic. For the segregated structure with an energy per particle of -2.230, the interplane separation of the porphyrins is large (approximately 12 Å) but still physically reasonable, and the packing fraction is only 0.12.

3.3 Simulations of the self-assembly process.

The self-assembly process of the oppositely charged porphyrins was investigated using two sets of starting structures: (a) those with randomly oriented porphyrins (derived from extended NVT runs of the ordered lattice structures at high temperatures), and (b) ordered lattice structures, particularly the segregated structure shown in Figure 5a. The goal of these studies was to investigate if it was possible to generate an ordered lattice from a randomly oriented structure or to transition between different lattice structures.

NVT studies of the random structures did not result in the formation of lattice structures, although a degree of local order was observed in some cases. In particular, portions of many simulations displayed ribbon-like structure with alternating oppositely charge porphyrins (see Figure 6). NpT studies beginning with a random structure also did not result in the formation of ordered lattices. The formation of a different and more stable lattice was observed when the segregated structure (E = -2.230 per particle) was used as a starting point in the NVT runs (Figure 7). The final structure showed the principal elements of the interleaved structure, usually with some slight slippage between layers. The energy of the final structure in Figure 6 (-3.057) did not match that of the fully interleaved structure (-3.295), presumably due to the fact that the simulation box contains several ordered regions separated by voids, preventing the full lattice energy from being realized.

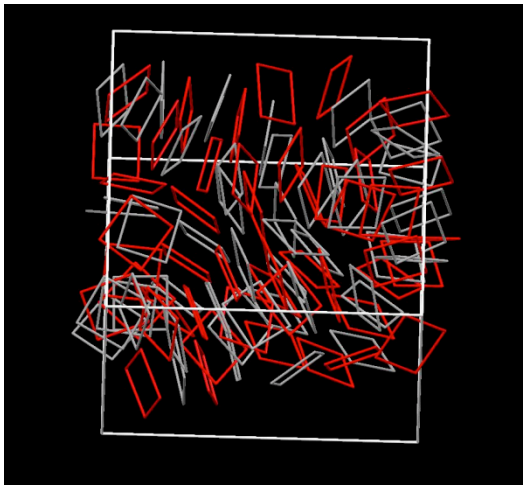

Figure 6. 'Ribbon'-type structures formed by oppositely charged porphyrins.

The transition from a segregated to interleaved structure was striking so additional simulations were performed to further investigate this change. A range of packing fractions were investigated to determine if this affected the segregated to interleaved transition. Significantly, interleaved structures were not generated with packing fractions of 0.10 or 0.16, indicating that the transition only occurs over a very narrow range of packing fractions. The structures formed at these higher or lower packing fractions were highly disordered. The segregated to interleaved transition was seen for large lattice simulations than those shown in Figure 7 (N = 192, consisting of a 2 x 2 x 6 lattice of unit cells each containing 8 molecules). The largest simulation attempted was for a 6 x 6 x 6 lattice corresponding to N = 1728 particles, where the simulation gave basically two fully interleaved phases separated by a void and the energy per particle (-3.14) was closer to that seen for the fully interleaved structure

4. CONCLUSIONS

A new class of solids, so-called binary ionic solids, has been successfully grown in the laboratory. The materials form as a range of nano- or micro-sized clovers with a morphology that depends on, among other things, the acidity of the solution. However, up until now the internal arrangement of the ionic macrocycles, although crucial to their function and future applications, is unfortunately virtually unknown. To gain insights into the internal structures of these materials

we have developed a model of nonconvex charge-decorated particles that interact through short-ranged Yukawa potentials. The self-assembly behavior and internal structures can be simulated with Monte Carlo techniques. This novel approach enables the first predictive simulation of these unusual binary ionic solids.

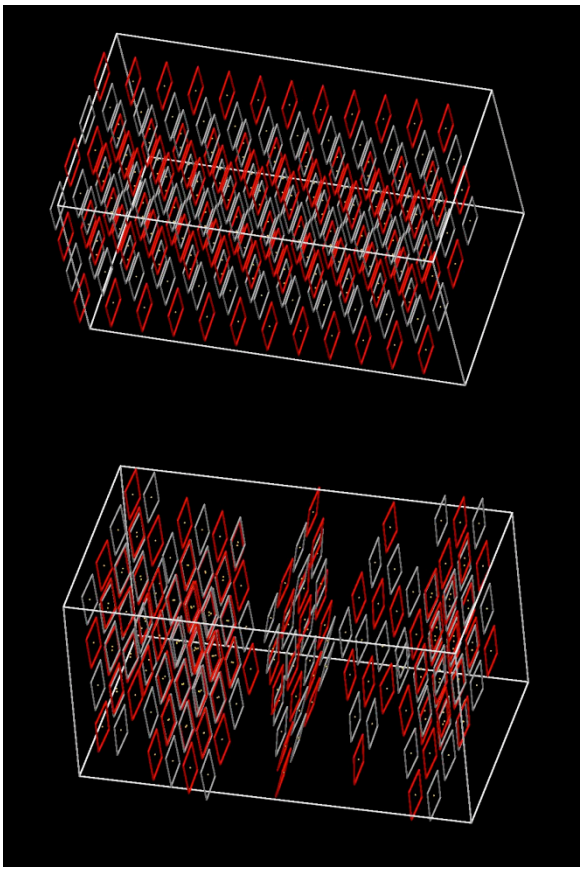

Figure 7. Starting segregated structure (N = 192, xsi = 0.12, E = -2.230 per particle) and final interleaved structure (E = -3.057). The simulation conditions were T = 0.005, electrostatic cutoff = 1.7, number of moves 1.68 x 10^7.

5. REFERENCES

1. Everything Mac, Apple Inc., **2010**
2. Larsen, B.; Monte Carlo Simulations on a charged hard sphere model, **1974**, *Chem. Phys. Lett*., 27, 47
3. van Swol, F., and Woodcock, L.V., to be published, **2010**
4. Allen, F. H., "*The Cambridge Structural Database: a quarter of a million crystal structures and rising*", *Acta Cryst.* **2002**, *B58*, 380.
5. Martin, K. E.; Wang, Z.; Busani, T.; Garcia, R. M.; Chen, Z.; Jiang, Y.; Song, Y.; Jacobsen, J. L.; Vu, T. T.; Schore, N. E.; Swartzentruber, B. S.; Medforth, C. J.; Shelnutt, J. A., "*Donor-Acceptor Biomorphs from the Ionic Self-Assembly of Porphyrins*", *J. Am. Chem. Soc.* **2010**, *132*, 8194.
6. Medforth, C. J.; Wang, Z.; Martin, K. E.; Song, Y.; Jacobsen, J. L.; Shelnutt, J. A., "*Self-Assembled Porphyrin Nanostructures*", *Chem. Commun.* **2009**, 7261 (Invited Review).
7. Medforth, C. J.; Shelnutt, J. A. "*Self-Assembled Porphyrin Nanostructures*", In *Handbook of Porphyrin Science*; Kadish, K. M., Smith, K. M., Guilard, R., Eds.; World Scientific Publishing: Hackensack, NJ, **2010**; Vol. 11 (Invited Review).

DISTRIBUTION

1 University of New Mexico
Attn: Prof. C. J. Medforth
University Blvd, Suite 100
Albuquerque, NM 87106

1	MS0824	Joel S. Lash	1510
1	MS1349	John A. Shelnutt	1815
1	MS1411	R. Allen Roach	1814
1	MS1411	Frank B. van Swol	1814
1	MS1349	William F. Hammetter	1815

1	MS0899	Technical Library	9536 (electronic copy)
1	MS0359	D. Chavez, LDRD Office	1911 (electronic copy


Sandia National Laboratories